Supplementary information

Towards highly loaded and finely dispersed CuO catalysts via ADP: Effect of the alumina support

Tim Van Everbroeck[a], Aggeliki Papavasiliou[b,*], Radu-George Ciocarlan[a], Evangelos Poulakis[c], Constantine J. Philippopoulos[c], Erika O. Jardim[d], Joaquin Silvestre-Albero[d], Pegie Cool[a], Fotis K. Katsaros[b]
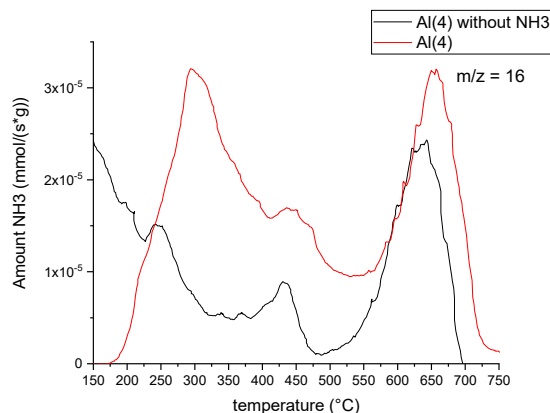
*Figure S1: NH$_3$-TPD and TPD after cleaning with He for **2 hours***
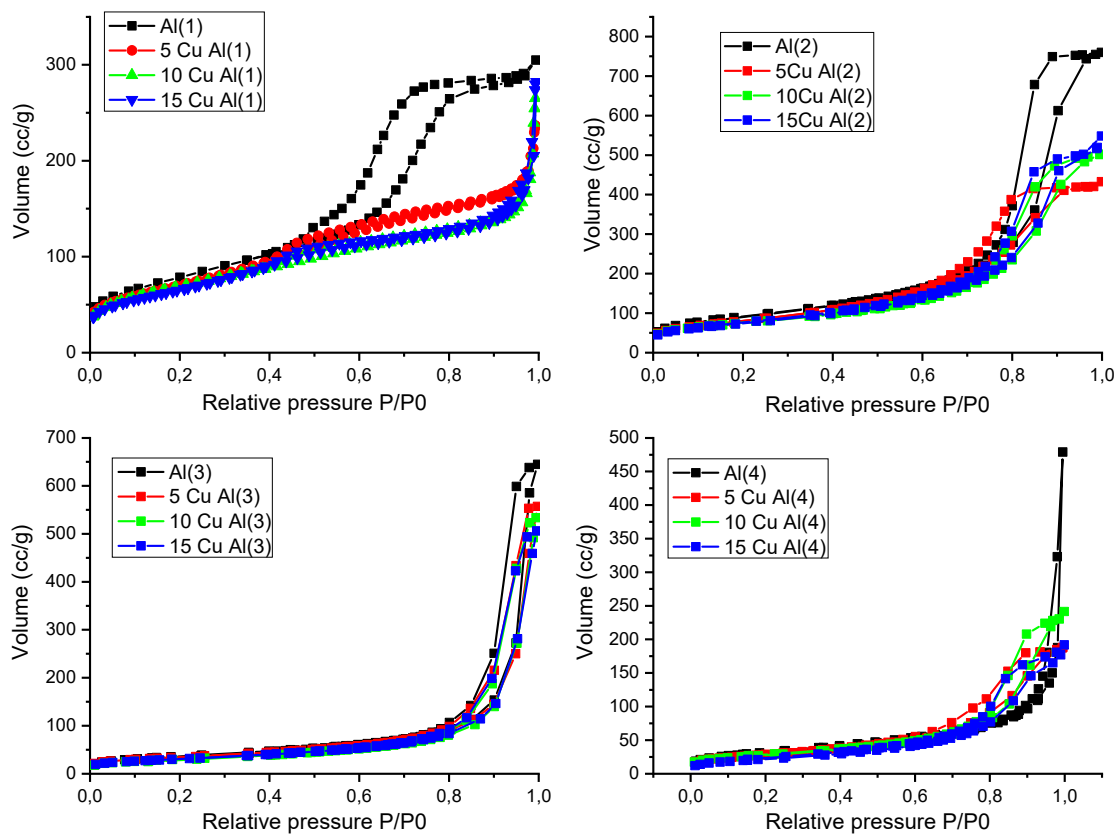
Figure S2: N$_2$-physisorption isotherms. Top left: Al(1) and derived materials loaded with CuO, top right: Al(2) and derived materials loaded with CuO, bottom left: Al(3) and derived materials loaded with CuO, bottom right: Al(4) and derived materials loaded with CuO
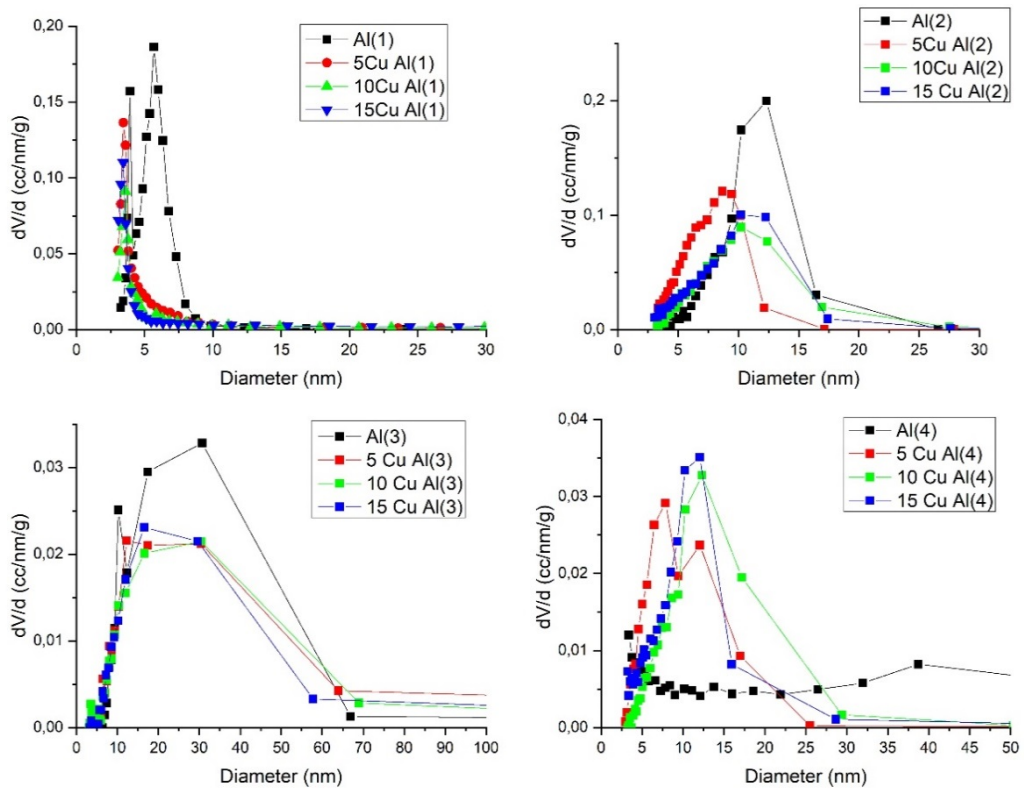
Figure S3: Pore-size distributions (PSD) derived from the desorption branch. Top left: Al(1) and derived materials loaded with CuO, top right: Al(2) and derived materials loaded with CuO, bottom left: Al(3) and derived materials loaded with CuO, bottom right: Al(4) and derived materials loaded with CuO
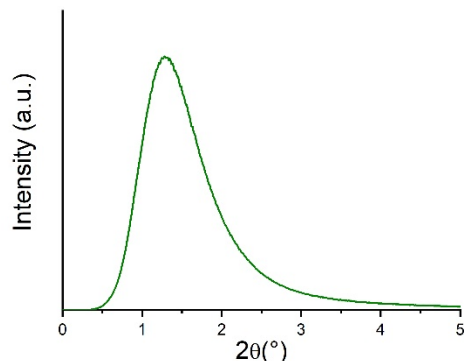

*Figure S4: Low angle XRD pattern of 5 Cu Al(1)*
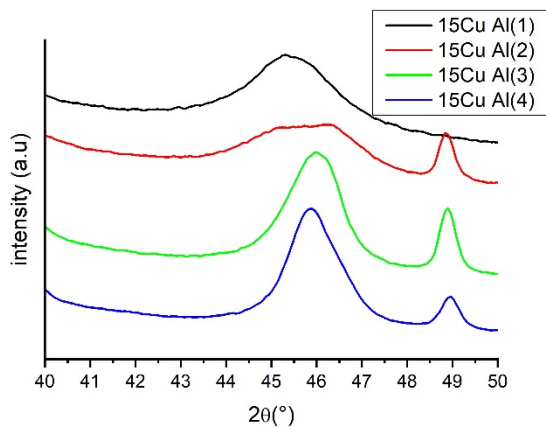
*Figure S5: Detail of the XRD patterns of the 15 wt% Cu loaded alumina samples*
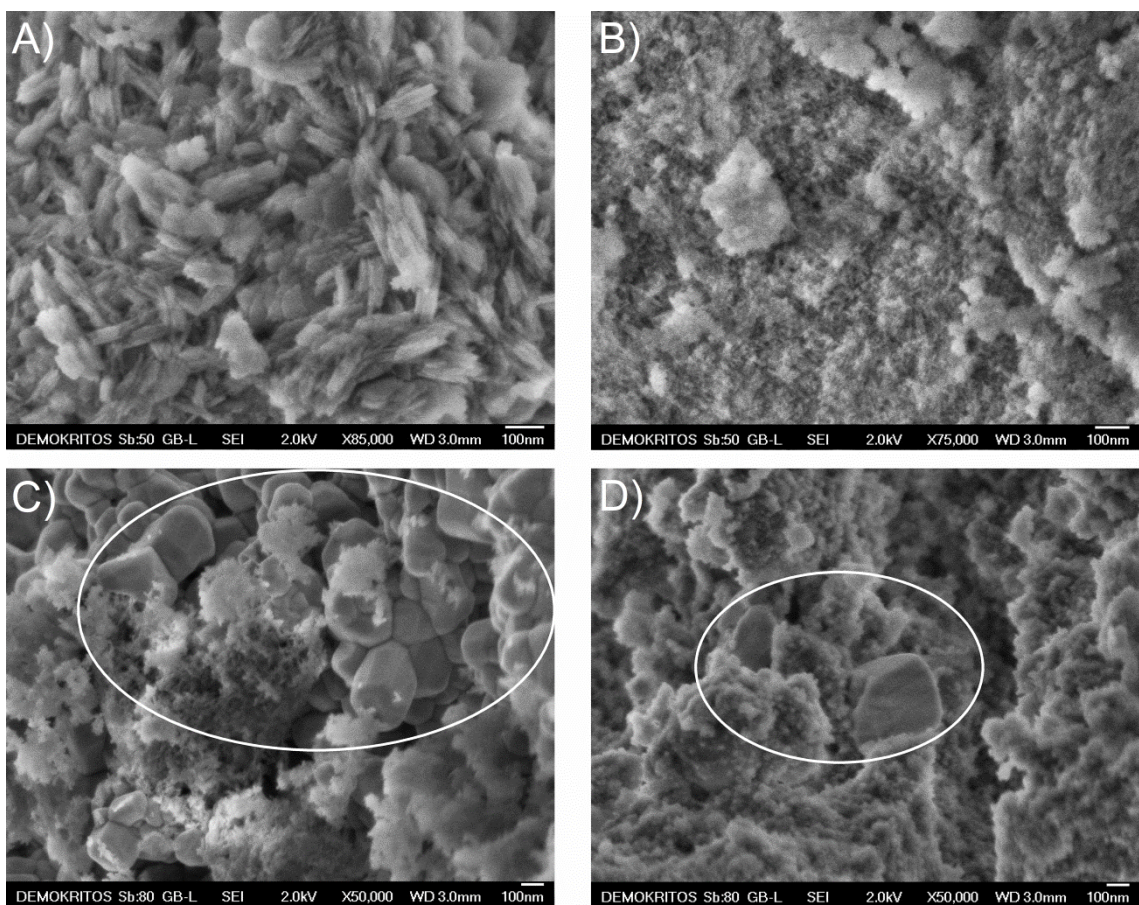
*Figure S6: SEM micrographs of A) 10Cu Al(1), B) 10Cu Al(2), C) 10Cu Al(3) and D) 10Cu Al(4) samples*
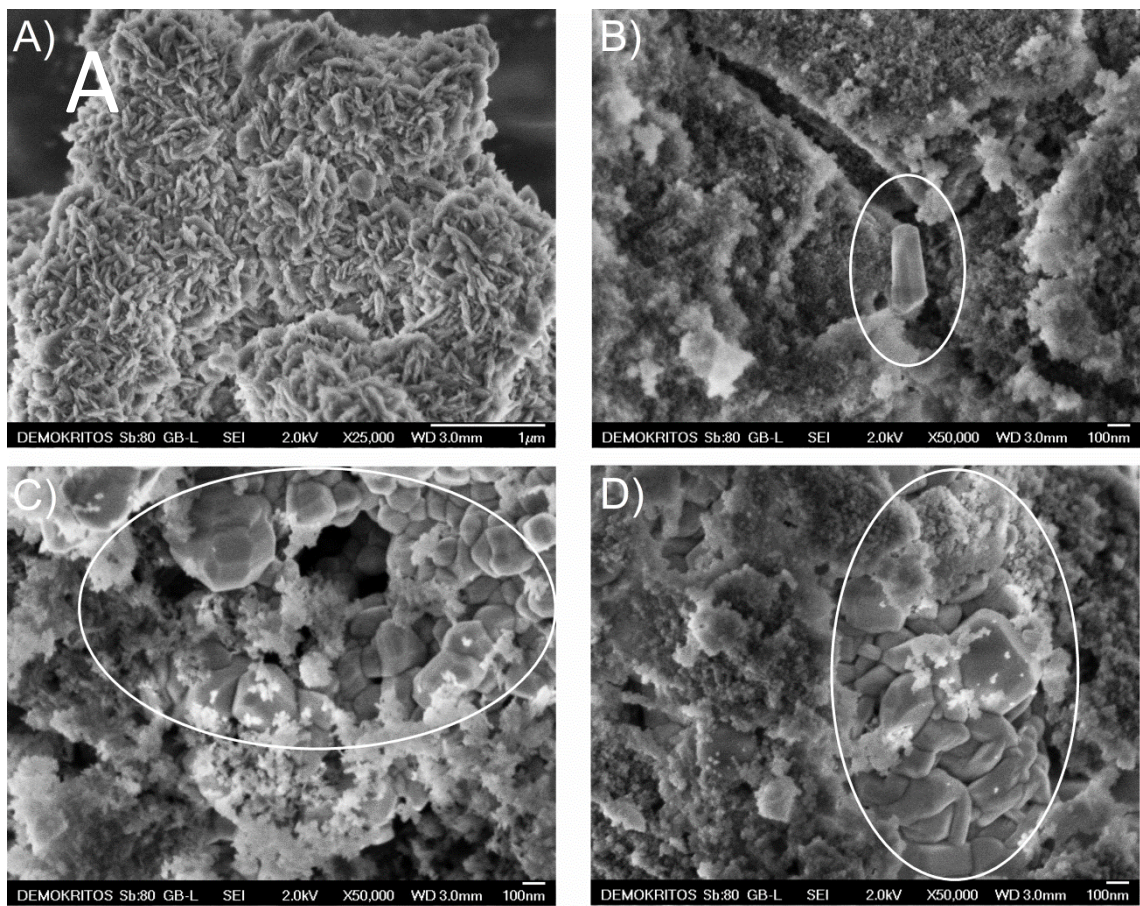
Figure S7: SEM micrographs of A) 15CuAl(1), B) 15CuAl(2), C) 15CuAl(3) and D) 15CuAl(4) samples
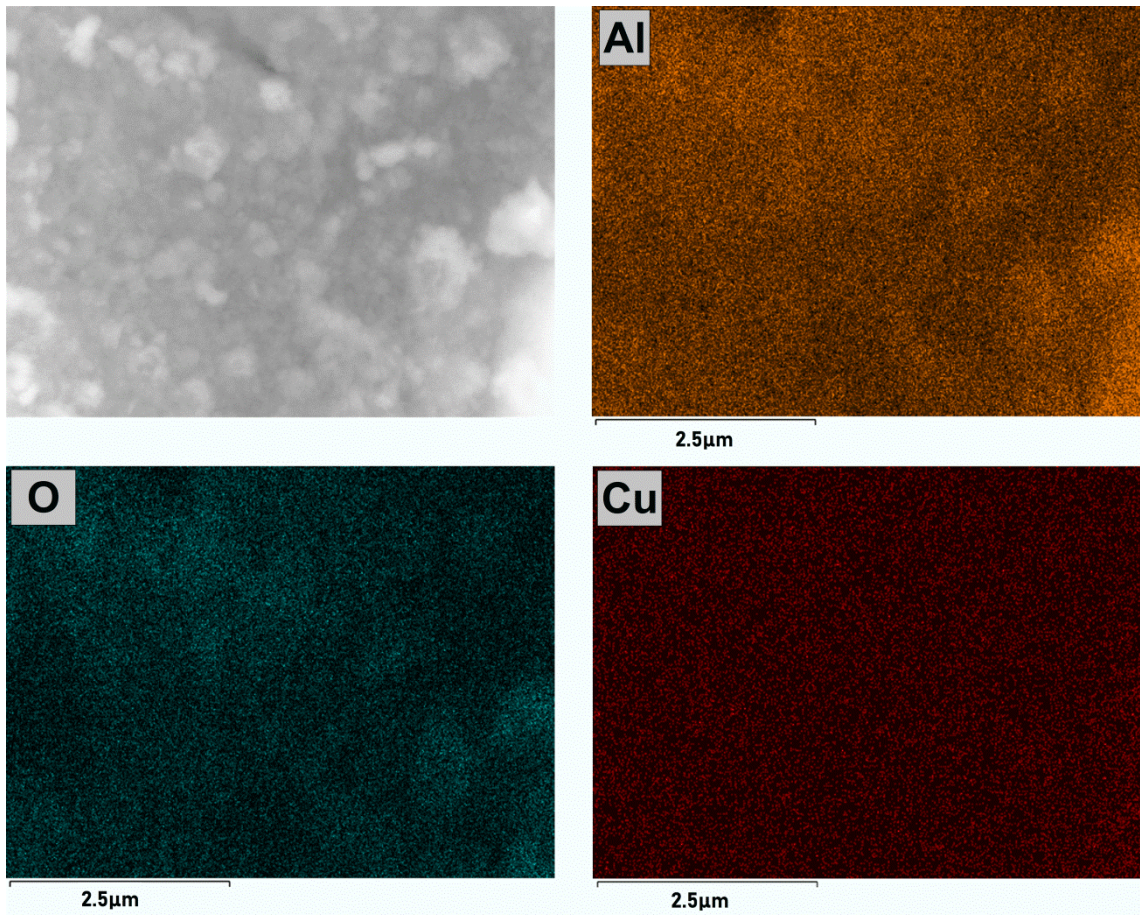
Figure S8: SEM micrograph of 5CuAl(1) sample and the corresponding O, Cu, Al elemental maps
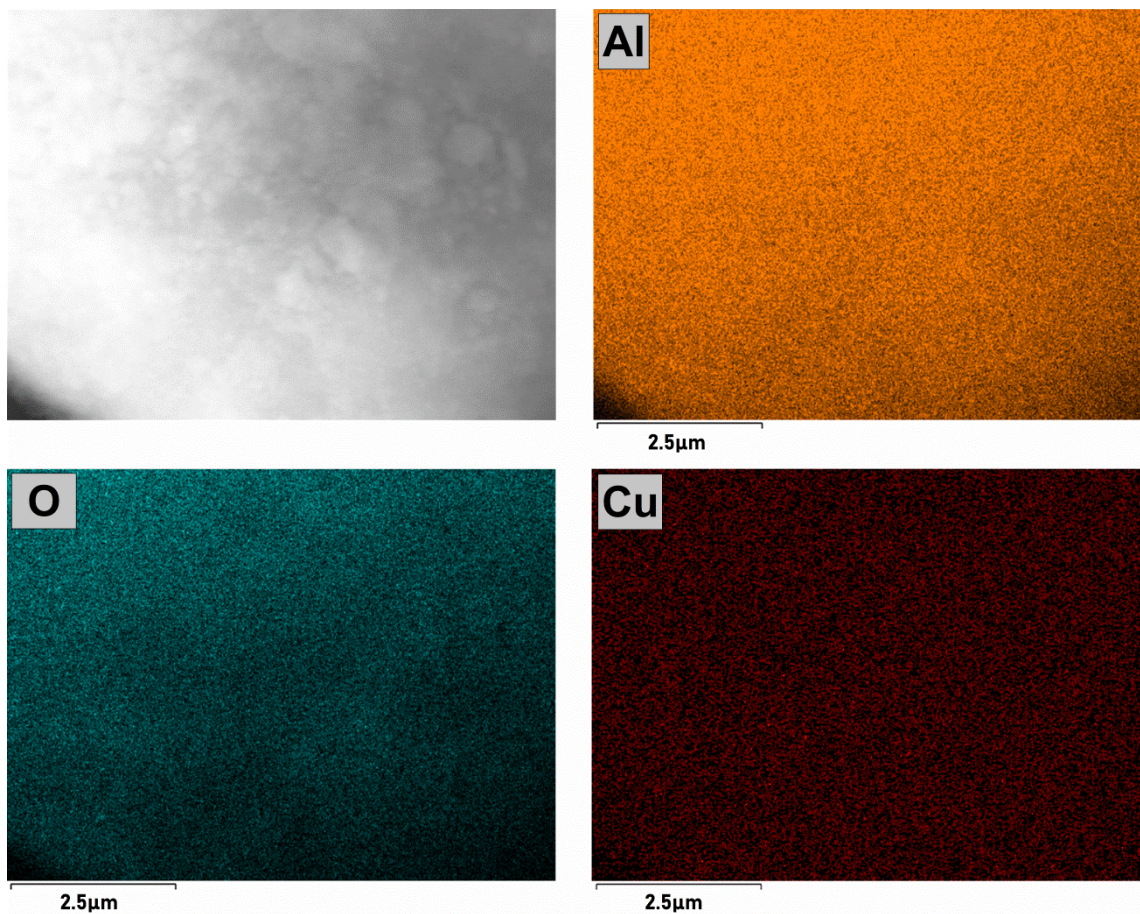
Figure S9: SEM micrograph of 5CuAl(2) sample and the corresponding O, Cu, Al elemental maps
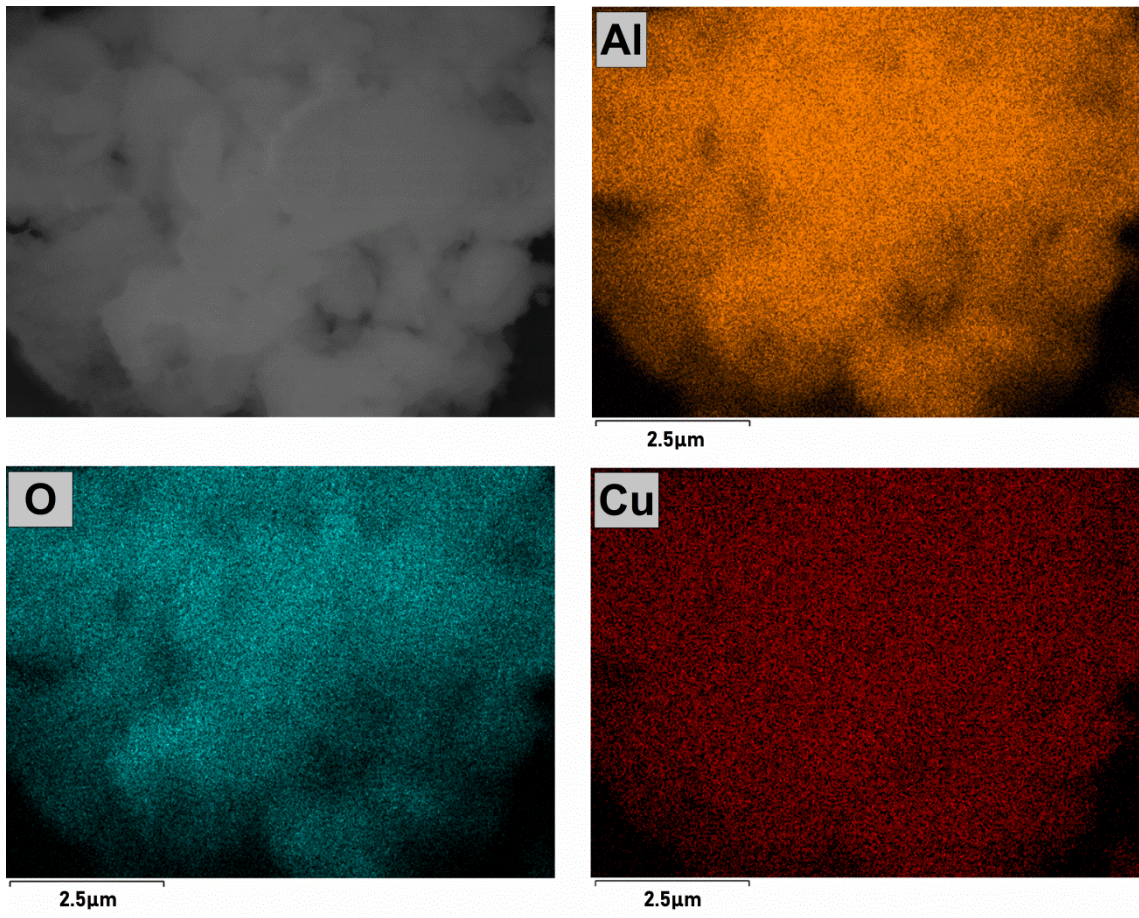
Figure S10: SEM micrograph of 15CuAl(1) sample and the corresponding O, Cu, Al elemental maps
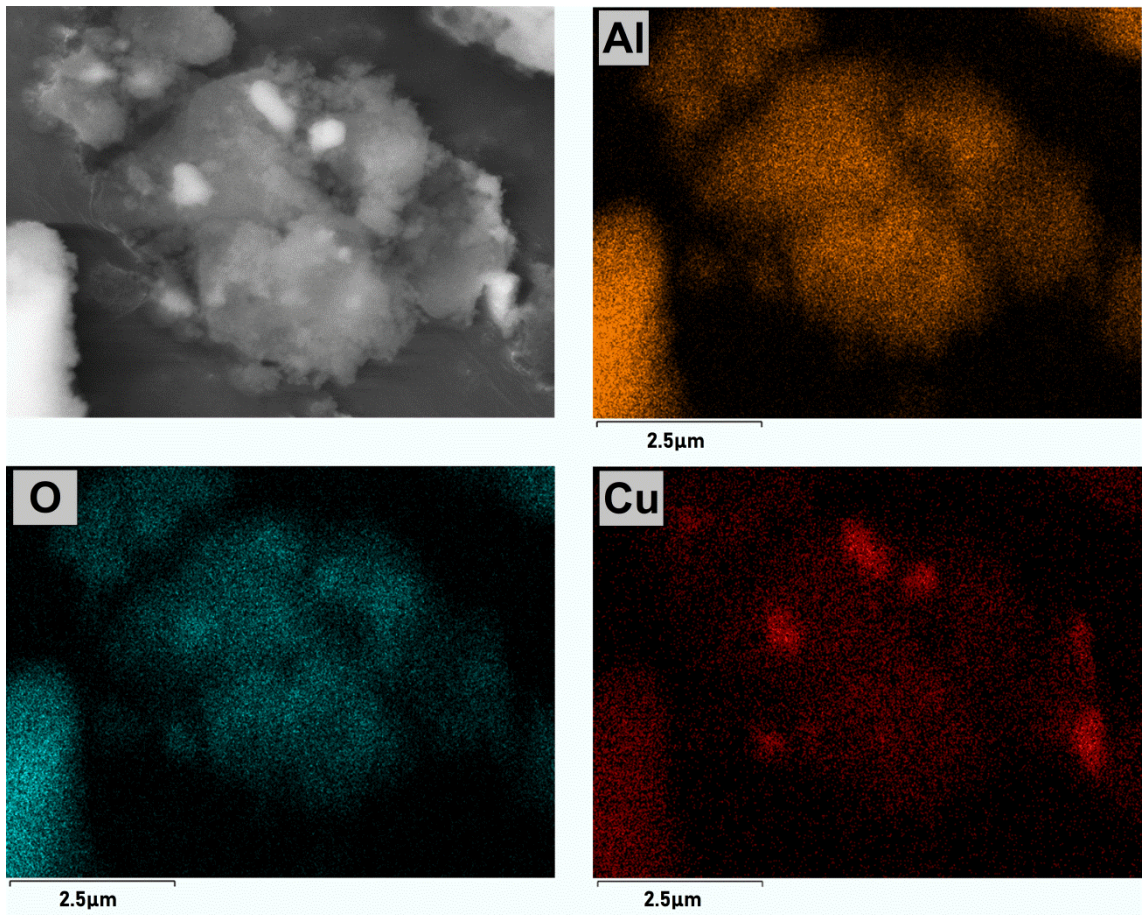
*Figure S11: SEM micrograph of 15CuAl(2) sample and the corresponding O, Cu, Al elemental maps*
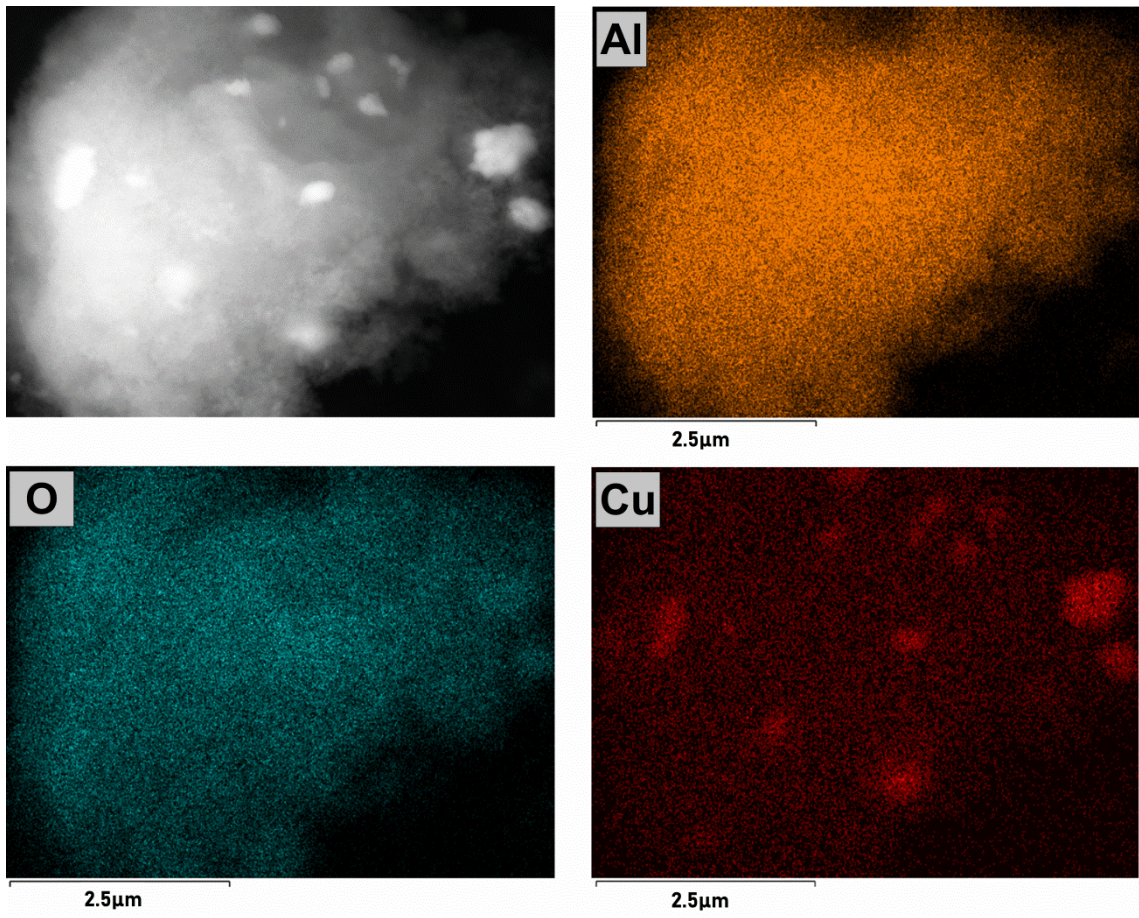
Figure S12: SEM micrograph of 15CuAl(3) sample and the corresponding O, Cu, Al elemental maps
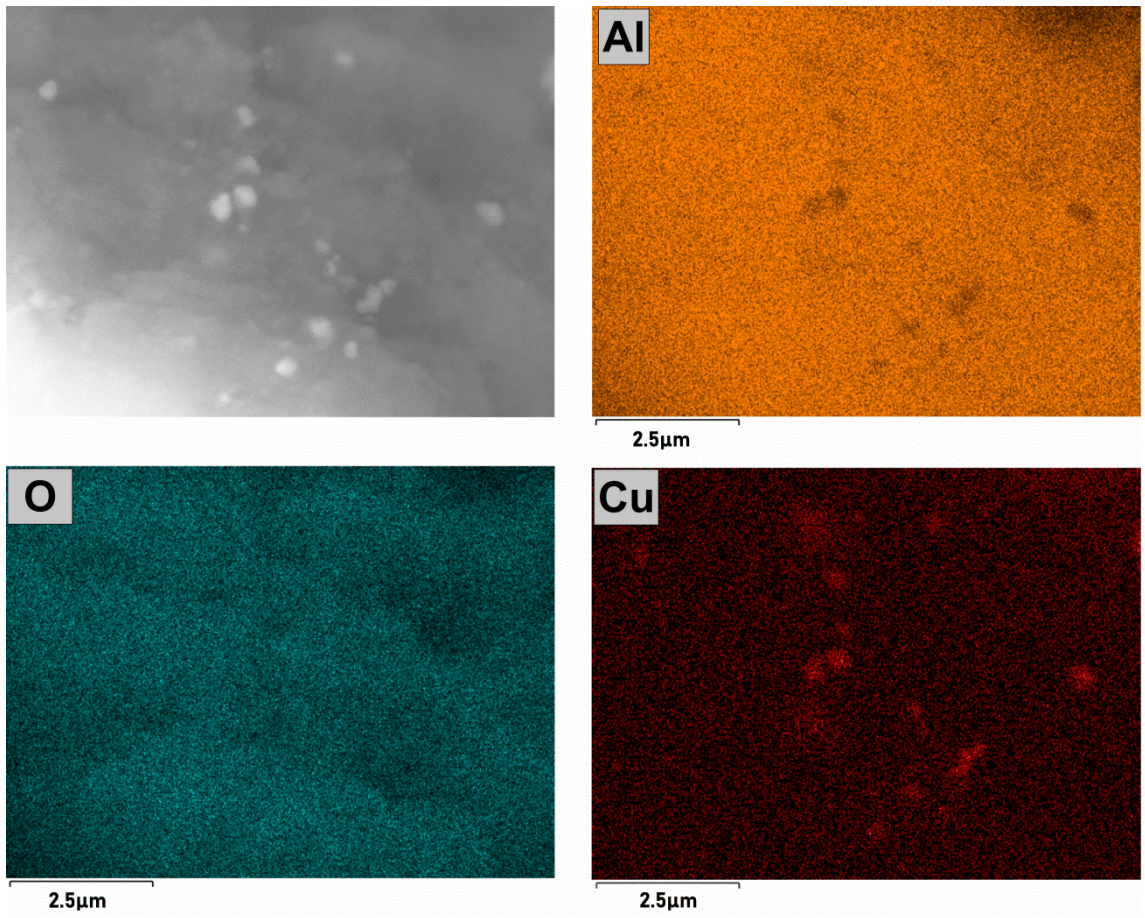
Figure S13: SEM micrograph of 15CuAl(4) sample and the corresponding O, Cu, Al elemental maps
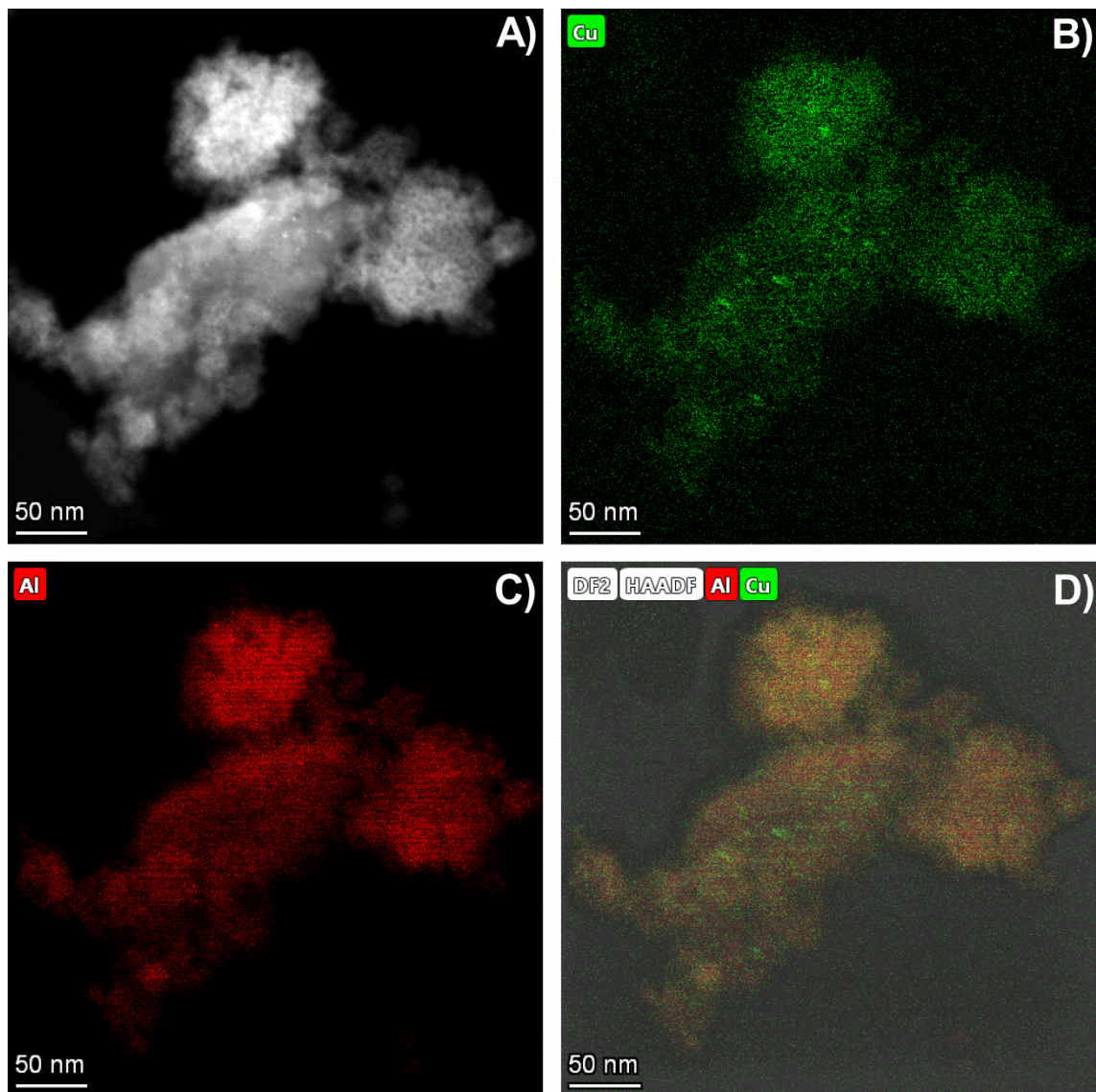
*Figure S14: A) HAADF STEM image and B-D) EDS mapping images of 5CuAl(1) sample*
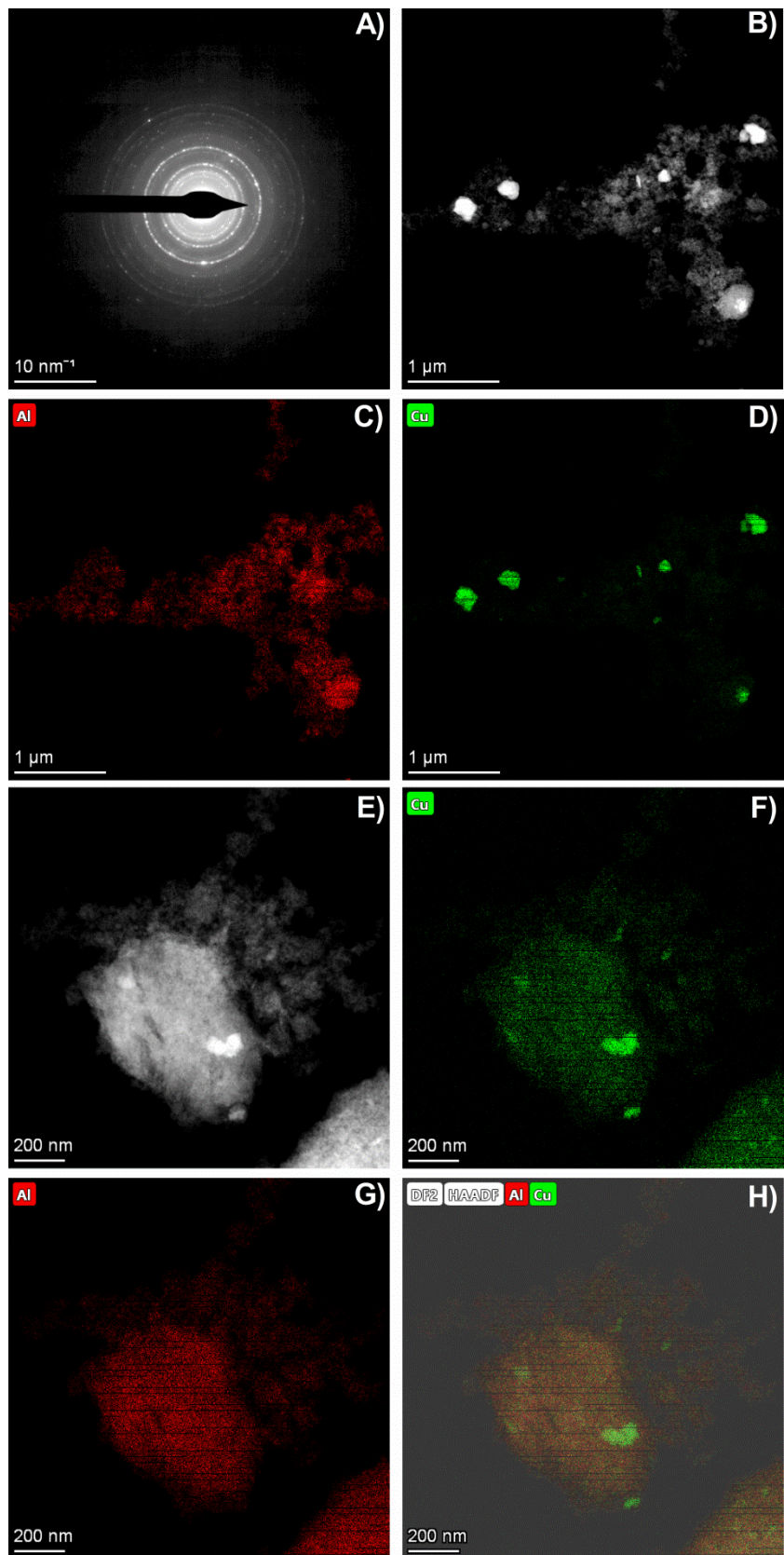
Figure S15: A) SAED pattern, B) HAADF STEM image, C-D) EDS mapping images of 15CuAl(4) sample, E) HAADF STEM image and F-H) EDS mapping images of 15CuAl(2) sample

13
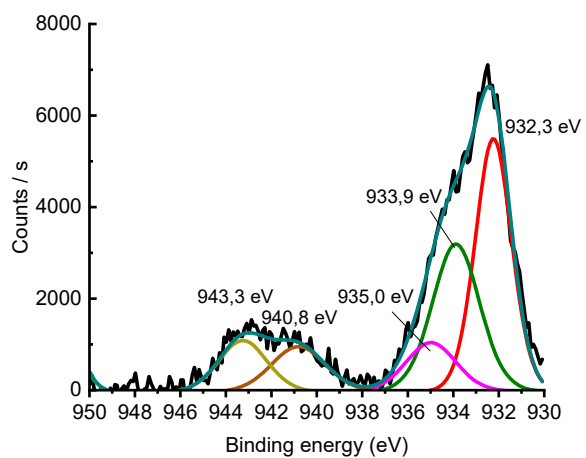
Figure S16: XPS characterisation of the Cu 2p$_{3/2}$ transition for 5 Cu Al(1) sample
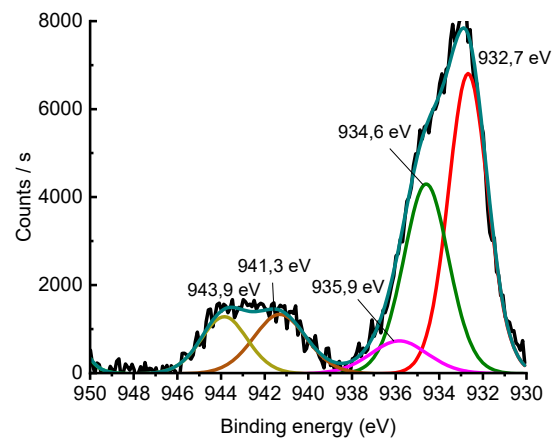
Figure S17: XPS characterization of the Cu 2p$_{3/2}$ transition for 5 Cu Al(2) sample
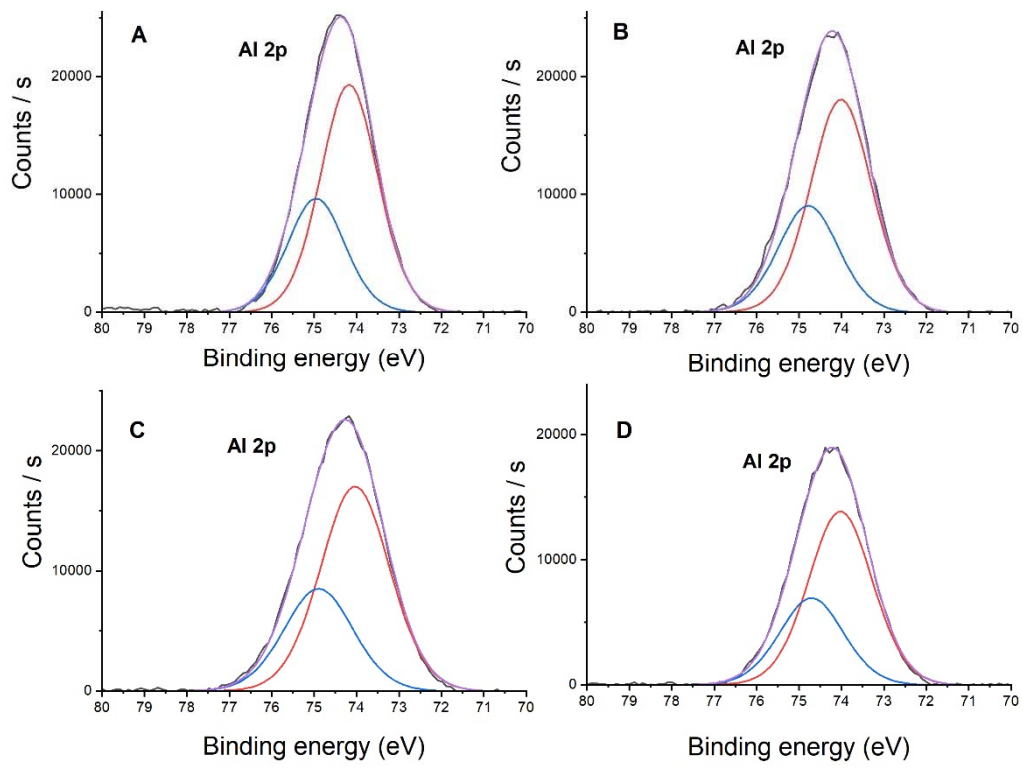
Figure S18: XPS characterization of the Al 2p transition for A) 15 Cu Al(1) B) 15 Cu Al(2) C) 15 Cu Al(3) D) 15 Cu Al(4)

The Al 2p transitions of the 15 wt% Cu loaded samples are shown in the supplementary information (Figure S 8). The Al 2p transition in γ-Al2O3 is reported to be at 73.5 eV [1], while for $CuAl_2O_4$ it is reported at 74.5 eV[2]. The Al2p XP spectra are rather similar for the four samples evaluated. For all catalysts there is a broad contribution at around 74.2-74.4 eV that can be deconvoluted in two peaks centered at 74.1 eV due to Al2p3/2 and 75.0 eV due to Al2p1/2. The shift in the binding energy of the Al2p contribution to higher values compared to γ-Al_2O_3 (73.5 eV) could be related either to $CuAl_2O_4$ spinel formation [1], or to the large number of alumina surface defect sites strongly interacting with CuO species[3].
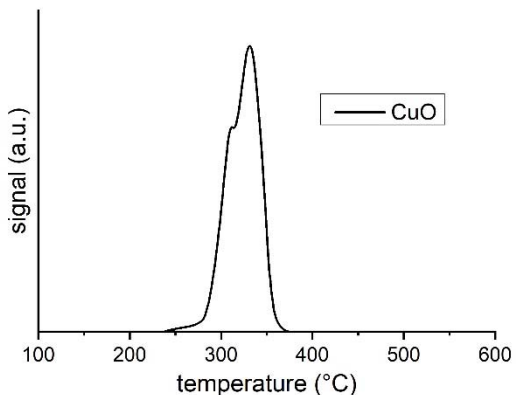
Figure S19: H₂-TPR profile of CuO
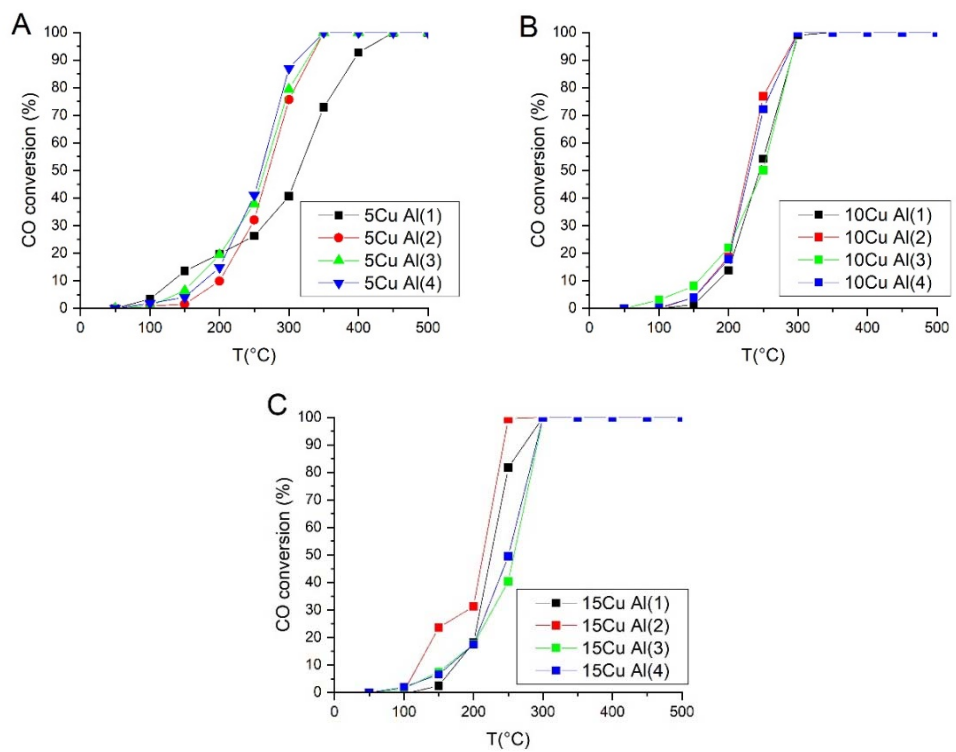
Figure S20: CO conversion profiles vs. temperature A) 5 wt% Cu loaded samples B) 10 wt% Cu loaded samples C) 15 wt% Cu loaded samples
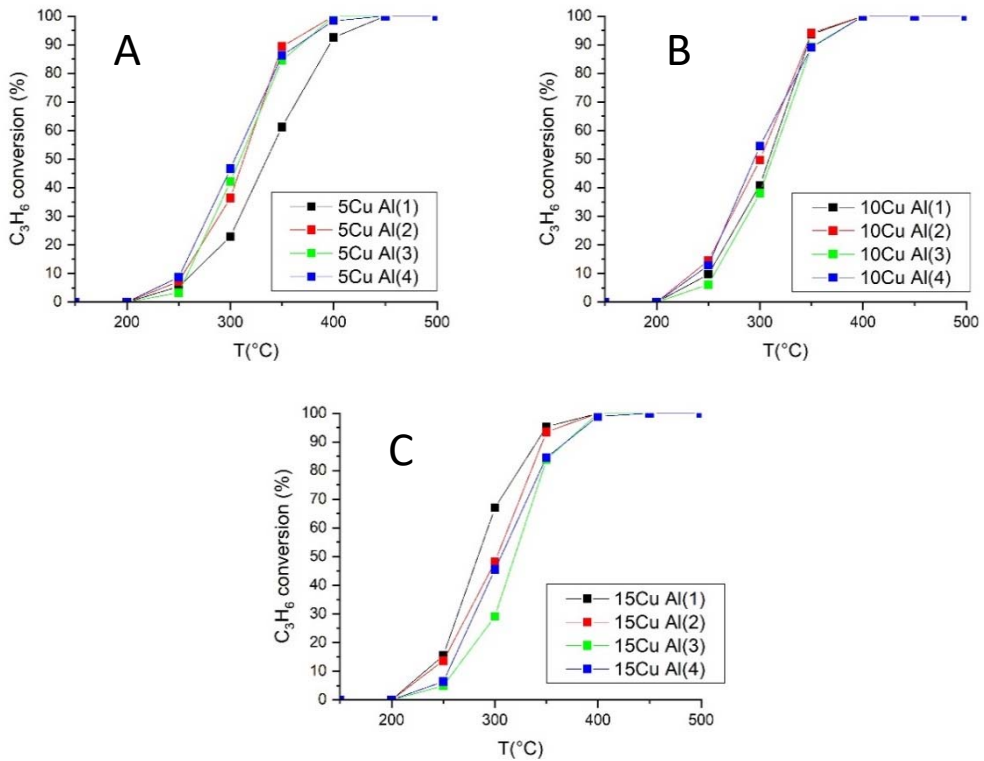
Figure S21: C₃H₆ conversion profiles vs. temperature A) 5 wt% Cu loaded samples B) 10 wt% Cu loaded samples C) 15 wt% Cu loaded samples
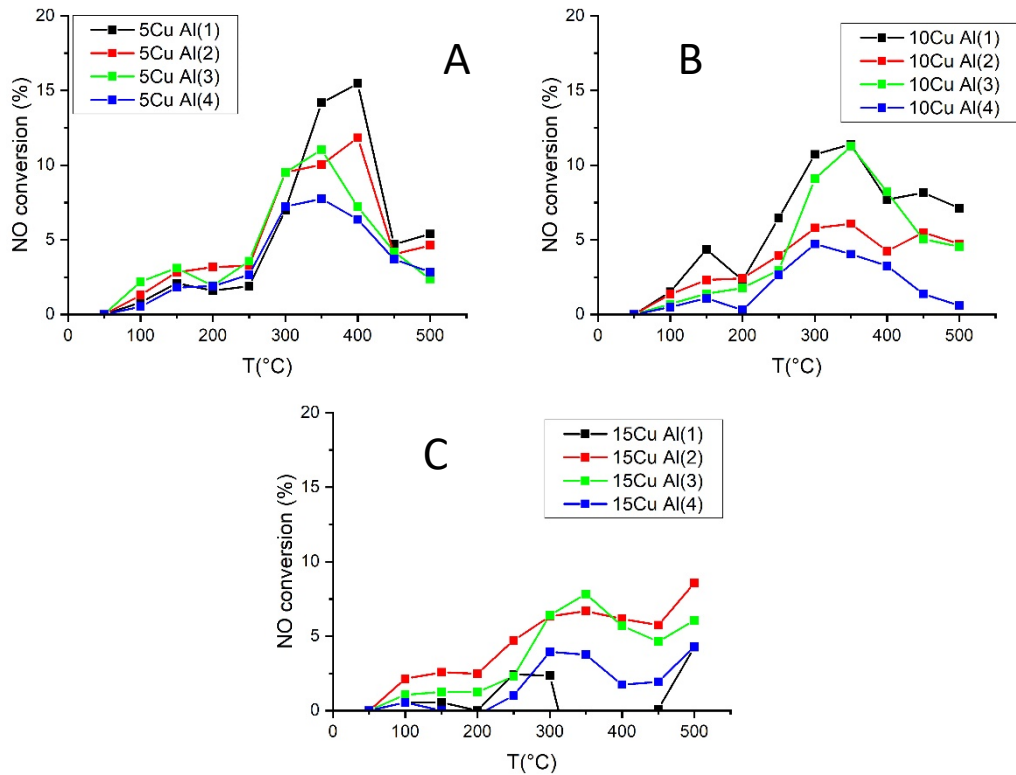
*Figure S22: NO conversion profiles vs. temperature A) 5 wt% Cu loaded samples B) 10 wt% Cu loaded samples C) 15 wt% Cu loaded samples*
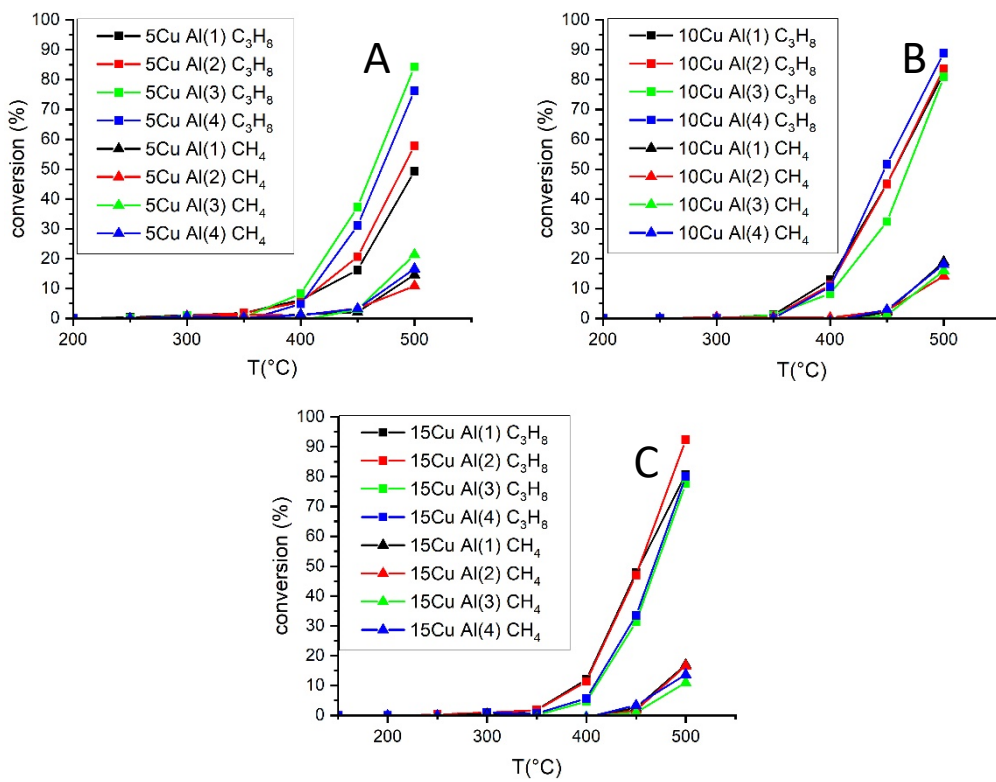
Figure S23: C$_3$H$_8$ and CH$_4$ conversion profiles vs. temperature A) 5 wt% Cu loaded samples B) 10 wt% Cu loaded

samples C) 15 wt% Cu loaded samples

		NO	CO	C$_3$H$_6$	C$_3$H$_8$	CH$_4$
5Cu Al(1)	T$_{50}$ (°C)	-	314	335	-	-
	T$_{90}$/T$_{max}$ (°C)	400	393	396	500	500
	Max. conv.(%)	15.5	100	100	49.4	14.6
5Cu Al(2)	T$_{50}$ (°C)	-	271	313	489	-
	T$_{90}$/T$_{max}$ (°C)	400	329	353	500	500
	Max. conv.(%)	11.8	100	100	57.9	10.9
5Cu Al(3)	T$_{50}$ (°C)	-	265	309	464	-

	T_{90}/T_{max} (°C)	350	326	368	500	500
	Max. conv.(%)	11	100	100	84.3	21.4
5Cu Al(4)	T_{50} (°C)	-	260	304	471	-
	T_{90}/T_{max} (°C)	350	311	366	500	500
	Max. conv.(%)	7.7	100	100	76.3	16.6
10Cu Al(1)	T_{50} (°C)	-	245	309	457	-
	T_{90}/T_{max} (°C)	350	290	347	500	500
	Max. conv.(%)	11.4	100	100	82.1	18.9
10Cu Al(2)	T_{50} (°C)	-	227	300	457	-
	T_{90}/T_{max} (°C)	350	278	345	500	500
	Max. conv.(%)	6.1	100	100	83.7	14.2
10Cu Al(3)	T_{50} (°C)	-	250	312	468	-
	T_{90}/T_{max} (°C)	350	290	354	500	500
	Max. conv.(%)	11.3	100	100	80.9	16
10Cu Al(4)	T_{50} (°C)	-	230	295	448	-
	T_{90}/T_{max} (°C)	300	282	355	500	500
	Max. conv.(%)	4.7	100	100	88.9	18.1
15Cu Al(1)	T_{50} (°C)	-	225	283	453	-
	T_{90}/T_{max} (°C)	500	273	341	500	500
	Max. conv.(%)	4.2	100	100	80.8	17
15Cu Al(2)	T_{50} (°C)	-	213	302	453	-
	T_{90}/T_{max} (°C)	500	243	346	500	500
	Max. conv.(%)	8.6	100	100	92.4	16.6
15Cu Al(3)	T_{50} (°C)	-	258	319	470	-

	T_{90}/T_{max} (°C)	350	292	369	500	500
	Max. conv.(%)	7.8	100	100	77.7	11
15Cu Al(4)	T_{50} (°C)	-	250	306	468	-
	T_{90}/T_{max} (°C)	500	290	369	500	500
	Max. conv.(%)	4.3	100	100	80	13.7

Table S1: Maximum conversion values, Light-off Temperatures (T_{50}), Temperatures of 90% conversion in case of CO and C_3H_6 and Temperatures of max conversion in case of C_3H_8, CH_4 and NO for the different tested catalysts

References:

[1]   G. Ertl, R. Hierl, H. Knözinger, N. Thiele, H.P. Urbach, XPS study of copper aluminate catalysts, Appl. Surf. Sci. (1980). https://doi.org/10.1016/0378-5963(80)90117-8.

[2]   F. Severino, J.L. Brito, J. Laine, J.L.G. Fierro, A.L. Agudo, Nature of Copper Active Sites in the Carbon Monoxide Oxidation on CuAl2O4and CuCr2O4Spinel Type Catalysts, J. Catal. 177 (1998) 82–95. https://doi.org/10.1006/JCAT.1998.2094.

[3]   H. Ham, J. Kim, S.J. Cho, J.H. Choi, D.J. Moon, J.W. Bae, Enhanced Stability of Spatially Confined Copper Nanoparticles in an Ordered Mesoporous Alumina for Dimethyl Ether Synthesis from Syngas, ACS Catal. (2016). https://doi.org/10.1021/acscatal.6b00882.